MOLECULAR PHARMACOLOGY
Vol. 66, No. 6
5827/1185835

Mol Pharmacol 66:1453–1464, 2004
Printed in U.S.A.

Single-Cell Imaging of Intracellular Ca^{2+} and Phospholipase C Activity Reveals That RGS 2, 3, and 4 Differentially Regulate Signaling via the $G\alpha_{q/11}$-Linked Muscarinic M_3 Receptor

Stephen C. Tovey and Gary B. Willars

Department of Cell Physiology and Pharmacology, University of Leicester, Leicester, United Kingdom

Received August 5, 2004; accepted September 17, 2004

ABSTRACT

Using single cell, real-time imaging, this study compared the impact of members of the B/R4 subfamily of the regulators of G-protein signaling (RGS) (RGS2, -3, and -4) on receptor-mediated inositol 1,4,5-trisphosphate [Ins(1,4,5)P_3], diacylglycerol, and Ca^{2+} signaling. In human embryonic kidney (HEK) 293 cells expressing recombinant $G\alpha_{q/11}$-coupled muscarinic M_3 receptors, transient coexpression of RGS proteins with fluorescently-tagged biosensors for either Ins(1,4,5)P_3 or diacylglycerol demonstrated that RGS2 and 3 inhibited receptor-mediated events. Although gross indices of signaling were unaffected by RGS4, it slowed the rate of increase in Ins(1,4,5)P_3 levels. At equivalent levels of expression, *myc*-tagged RGS proteins showed inhibitory activity on the order RGS3 ≥ RGS2 > RGS4. In HEK293 cells, stable expression of *myc*-tagged RGS2, -3, or -4 at equivalent levels also inhibited phosphoinositide and Ca^{2+} signaling by endogenously expressed muscarinic M_3 receptors in the order RGS3 ≥ RGS2 > RGS4. In these cells, RGS2 or -3 reduced receptor-mediated inositol phosphate generation in cell populations and reduced both the magnitude and kinetics (rise-time) of single cell Ca^{2+} signals. Furthermore, at low levels of receptor activation, oscillatory Ca^{2+} signals were dampened or abolished, whereas at higher levels, RGS2 and -3 promoted the conversion of more stable Ca^{2+} elevations into oscillatory signals. Despite little or no effect on responses to maximal receptor activation, RGS4 produced effects on the magnitude, kinetics, and oscillatory behavior of Ca^{2+} signaling at submaximal levels that were consistent with those of RGS2 and -3.

The family of regulators of G-protein signaling (RGS) negatively regulate signaling by G-protein-coupled receptors (GPCRs) by binding to activated Gα-subunits and acting as either GTPase-activating proteins (GAPs) or effector antagonists (Hepler, 1999; Ross and Wilkie, 2000; Hollinger and Hepler, 2002). More than 30 distinct proteins are now known to exist that contain an RGS or RGS-like domain. This is an approximately 120-amino acid region through which these proteins can increase the intrinsic GTPase activity of GTP-bound Gα subunits. It is interesting that many RGS proteins contain other recognizable protein binding domains, such as the G-protein γ-like (RGS6, -7, -9, -11) (Snow et al., 1998a), which confers binding to the G-protein subunit Gβ5, PDZ (RGS12, PDZ-RhoGEF) (Snow et al., 1998b; Hollinger and Hepler, 2002), DEP (disheveled, Egl-10, pleckstrin) (RGS6, -7, -9, -11) (Snow et al., 1998a), DH (dbl homology) and PH (pleckstrin homology) domains (p115RhoGEF, PDZ-RhoGEF) (reviewed in Hollinger and Hepler, 2002). These domains may be involved in determining cellular localization and RGS specificity toward Gα subunits, and they may also confer signaling roles distinct from inhibition of Gα-subunits (Hollinger and Hepler, 2002).

RGS and RGS-like proteins have been classified into subfamilies based on the alignment of the RGS domain amino acid sequences (Zheng et al., 1999; Ross and Wilkie, 2000). According to this scheme, RGS2, -3, and -4 each belong to the B/R4 RGS subfamily, of which RGS4 is considered the prototypical member. Except for RGS3, the B/R4 subfamily are small proteins (20–30 kDa) that contain an N-terminal cat-

This work was supported financially by the Biotechnology and Biological Research Council (ref. 91/C15897) and the Wellcome Trust (ref. 061050).
Article, publication date, and citation information can be found at http://molpharm.aspetjournals.org.
doi:10.1124/mol.104.005827.

ABBREVIATIONS: RGS, regulators of G-protein signaling; GPCR, G-protein-coupled receptor; GAP, GTPase-activating protein; Ins(1,4,5)P_3, inositol 1,4,5-trisphosphate; eGFP, enhanced green fluorescent protein; HEK, human embryonic kidney; eGFP-$PH_{PLC\delta1}$ eGFP coupled to the pleckstrin homology domain of $PLC_{\delta1}$; eGFP-PKC$\gamma C1_2$ eGFP coupled to the diacylglycerol binding domain of the $C1_2$ region of PKCγ; HEK293/M_3, HEK293 cells expressing recombinant human muscarinic M_3 receptors; HEK293/RGS2*myc*, HEK293 cells expressing recombinant RGS2*myc*; HEK293/RGS3*myc*, HEK293 cells expressing recombinant RGS3*myc*; HEK293/RGS4*myc*, HEK293 cells expressing recombinant RGS4*myc*; PLC, phospholipase C; CA, constitutively active; WT, wild-type; TTBS, Tris-buffered saline/Tween 20; BSA, bovine serum albumin; PBS, phosphate-buffered saline; FITC, fluorescein isothiocyanate; KHB, Krebs-HEPES buffer; [^{3}H]InsP_x, ^{3}H-labeled mono- and polyphosphates of inositol; ANOVA, analysis of variance.

ionic amphipathic α-helix that, at least for RGS4, is responsible for membrane attachment. Although RGS3 also contains an amphipathic α-helix adjacent to its RGS domain, it is a relatively large (~70 kDa) protein with an N-terminal region three times larger than the RGS domain. The function of this N-terminal region, however, is poorly understood (Castro-Fernandez and Conn, 2002). RGS3 has previously been shown to inhibit signaling by several receptors [e.g., the $G\alpha_{q/11}$-coupled gonadotropin-releasing hormone receptor) (Castro-Fernandez and Conn, 2002; Neill et al., 1997). RGS4 has previously been shown to inhibit signaling by both $G\alpha_i$- and $G\alpha_{q/11}$-coupled receptors (e.g., the muscarinic M_2 and M_3 receptors, respectively) (Doupnik et al., 1997; Rumenapp et al., 2001). In contrast, RGS2 lacks GAP activity toward $G\alpha_i$, at least in vitro, but is 5- to 10-fold more potent than RGS4 in blocking $G\alpha_q$-mediated activation of phospholipase Cβ (Heximer et al., 1997).

Many previous studies that have assessed the impact of RGS protein expression on the function of $G\alpha_{q/11}$-coupled receptors have relied upon transient overexpression of RGS proteins and analysis of their effects in population-based assays (such as total inositol phosphate accumulation). The recent advent of novel biosensors to detect the generation of either inositol 1,4,5-trisphosphate [Ins(1,4,5)P_3] (eGFP-$PH_{PLC\delta1}$) or diacylglycerol (eGFP-PKC$\gamma C1_2$) has allowed examination of phospholipase C (PLC) activity at the single-cell level (Oancea and Meyer, 1998; Oancea et al., 1998; Stauffer et al., 1998; Nash et al., 2001). In particular, Ins(1,4,5)P_3 and diacylglycerol production can be determined at the single-cell level in real-time and at a spatial resolution previously unimaginable (Nahorski et al., 2003). The eGFP-$PH_{PLC\delta1}$ construct represents a fusion protein of enhanced green fluorescent protein (eGFP) with the pleckstrin homology domain of PLCδ1. At rest, eGFP-$PH_{PLC\delta1}$ is localized to the plasma membrane, where it binds with high affinity and selectivity to phosphatidylinositol 4,5-bisphosphate (Stauffer et al., 1998; Nash et al., 2001); upon agonist stimulation, however, it becomes cytosolic as Ins(1,4,5)P_3 is produced and binds to it with high affinity, thereby displacing it from the membrane (Nash et al., 2001). The eGFP-PKC$\gamma C1_2$ construct represents eGFP coupled to the diacylglycerol binding domain of the $C1_2$ region of PKCγ. Under resting conditions, it has a cytosolic localization, but upon agonist stimulation and diacylglycerol production, it is recruited to the plasma membrane (Oancea and Meyer, 1998; Oancea et al., 1998).

In the present study, we show for the first time that novel protein-based biosensors that detect Ins(1,4,5)P_3 and diacylglycerol production can be used to examine how RGS proteins differentially regulate $G\alpha_{q/11}$-mediated signaling via the muscarinic M_3 receptor at the single-cell level. Furthermore, we also show how RGS proteins differentially influence the pattern and kinetics of Ca^{2+} signaling at the single cell level.

Materials and Methods

Materials. Cell culture plasticware was from Nalge Nunc International (Roskilde, Denmark) and cell culture reagents were from Invitrogen (Paisley, UK). [*myo*-^{3}H]Inositol was from Amersham Biosciences (Little Chalfont, Buckinghamshire, UK). Unless stated otherwise, other reagents were supplied by either Sigma Aldrich (Poole, UK), Fisher Scientific (Loughborough, UK), Merck (Darmstadt, Germany), or BDH Laboratory Supplies (Poole, UK).

Original RGS DNA Constructs. Plasmids containing full-length constructs encoding human RGS2 (L13463), human RGS3 (U27655), and rat RGS4 (U27767) were gifts from Dr. Craig Doupnik (University of South Florida College of Medicine, Tampa, FL). The plasmids for RGS2 and RGS3 in the mammalian expression vector pRcCMV (Invitrogen) were originally from Drs. Kirk Druey and John Kehrl (National Institutes of Health, Bethesda, MD), whereas the plasmid for RGS4 in the mammalian expression vector pcDNA3.1 (Invitrogen) originated from Dr. Henry Lester (California Institute of Technology, Pasadena, CA). The plasmid containing a constitutively active $G\alpha_q$ mutant (Q209L) (CA-$G\alpha_q$) was a gift from Dr. Scott Heximer (University of Washington, St. Louis, MO) and originated from Dr. John Hepler (Emory University, Atlanta, GA). The vectors for the Ins(1,4,5)P_3 (eGFP-$PH_{PLC\delta1}$) and diacylglycerol (eGFP-PKC$\gamma C1_2$) biosensors were provided by Professor T. Meyer (Stamford University, Stanford, CA).

Generation of *myc*-Tagged Constructs. RGS2, -3, and -4 were PCR amplified from their original vectors to incorporate KpnI and XhoI restriction sites. The resulting PCR fragments were then column-purified (QIAGEN, Crawley, UK) and subcloned into pcDNA3.1/*myc*-His (Invitrogen). Expression of these constructs results in the generation of C-terminal *myc*-epitope-tagged RGS proteins.

Establishing Stable Muscarinic M_3 Expression in HEK293 Cells. The generation of HEK293 cells stably expressing the muscarinic M_3 receptor was achieved using a standard calcium phosphate method. Wild-type HEK293 cells (HEK293/WT) were transfected with the DNA encoding the human muscarinic M_3 receptor that had been cloned (BamHI/EcoRI) into the plasmid pcDNA3 (Invitrogen,). Cells were selected with Geneticin (G-418; 500 μg/ml), and clones were expanded from single foci. Muscarinic receptor expression was determined by the binding of the muscarinic receptor antagonist 1-[*N*-methyl-^{3}H]scopolamine methyl chloride exactly as described elsewhere (Willars et al., 1998a), and a single clone was selected for further study. These cells (HEK293/M_3 cells) express approximately 1.7 pmol of receptor/mg of protein compared with approximately 40 fmol of muscarinic receptor/mg of protein in HEK293/WT cells.

Cell Culture and Transfection. Both HEK293/M_3 and HEK293/WT cells were cultured in α minimal essential medium with GlutaMAX-1 and Earles' salts, supplemented with nonessential amino acids (1%), fetal calf serum (10%), and gentamicin (50 μg/ml). Cells were maintained in a humidified atmosphere (95% O_2/5% CO_2; 37°C) with the culture media replaced every third day and the cells passaged when they reached ~80% confluence. For single-cell imaging, cells were plated onto 25-mm borosilicate glass coverslips coated with 0.01% poly-D-lysine (Sigma, Poole, UK). After 2 days in culture, cells were transfected with the relevant DNA using Genejuice (Merck Bioscience, Nottingham, UK) at a Genejuice/DNA ratio of 3:1 according to the manufacturer's guidelines. Cells were used for imaging experiments 48 h after transfection.

Establishing Stable RGS*myc* Expression in HEK293 Cells. Stable RGS*myc*-expressing cell lines were made according to established protocols (Willars et al., 1998a). In brief, HEK293/WT cells were grown to ~50% confluence on 100-mm cell culture dishes. Cells were then transfected with 3 μg of RGS*myc* DNA using Genejuice as described above. After 48 h, transfected cells were selected using G-418 (500 μg/ml). Cells on transfected plates were allowed to grow until all cells on a control plate of untransfected cells had died. Transfected cells were then serially diluted and seeded into 96-well plates. Single colonies originating from individual cells were then selected and expanded for screening by Western blotting with an anti-*myc* antibody (New England Biolabs, Hitchin, UK). The stable expression of RGS*myc* proteins in selected clones was then confirmed throughout the experimental period using Western blotting.

Western Blotting of RGS*myc* Proteins. Cells grown in 24- or six-well plates were solubilized (10 mM Tris, 10 mM EDTA, 500 mM NaCl, 1% Igepal CA630, 0.1% SDS, 0.5% deoxycholate, 1 mM phenylmethylsulfonyl fluoride, 100 μg/ml iodoacetamide, and 100 μg/ml

benzamidine, pH 7.4) and proteins (~30 μg/lane) separated by SDS-polyacrylamide gel electrophoresis using 8 to 12% running gels. Proteins were transferred onto nitrocellulose membranes, which were then blocked for 1 h in 5% (w/v) nonfat dry milk in TTBS (137 mM NaCl, 20 mM Tris, pH 8.0, and 0.05% Tween 20, pH 8.0) and incubated overnight at 4°C with primary antibody against the *myc* epitope (New England Biolabs) at 1:1000 in 3% bovine serum albumin (BSA) in TTBS. Blots were then washed three times (for 10 min each) in TTBS and incubated for 1 h with an anti-rabbit horseradish peroxidase-conjugated secondary antibody (1:3000 in blocking buffer; Sigma). After three further washes in TTBS (10 min each), the blots were exposed to ECL Plus detection reagents (Amersham Biosciences) according to the manufacturer's guidelines, and bands were visualized using Hyperfilm (Amersham Biosciences).

Immunostaining of RGS*myc* Proteins. Cells were plated onto 22-mm diameter glass coverslips and allowed to adhere for 48 h before transfection. Immunostaining was carried out as described previously (Tovey et al., 2001). In brief, cells were washed with phosphate-buffered saline (PBS) and then immediately fixed for 30 min in 4% paraformaldehyde in PBS. After fixation, cells were permeabilized in PBS with 0.2% Triton-X100 (10 min); thereafter, nonspecific sites were blocked by a 45-min incubation with PBS containing 3% BSA and 0.2% Triton-X100. Cells were then incubated overnight at 4°C in primary antibody (anti-*myc*; 1:100 in PBS with 3% BSA). On the following day, cells were washed three times in PBS (10 min each) and then incubated for 1 h with an anti-rabbit FITC-conjugated secondary antibody (1:250 in PBS with 10% goat serum; Vector Labs, Peterborough, UK). After three further washes (10 min each) in PBS, coverslips were mounted onto microscope slides using Vectorshield Fluorescence Preservative (Vector Labs). FITC labeling was then visualized using a Fluoview confocal microscope (Olympus, Tokyo, Japan).

Confocal Imaging of eGFP-Tagged Biosensors and Intracellular Ca^{2+} Signals. Cells were transfected with eGFP-tagged biosensor DNA with or without RGS/RGS*myc* DNA 48 h before imaging as described above. In general, an individual well of a six-well multidish was transfected with 0.5 μg of biosensor DNA alone or cotransfected with 0.5 μg of biosensor DNA and an excess of RGS/RGS*myc* DNA (1.5 μg) to ensure that all cells transfected with biosensor were cotransfected with RGS/RGS*myc* DNA. Before imaging, the culture medium was replaced with a Krebs-HEPES buffer (KHB) [10 mM HEPES, 4.2 mM $NaHCO_3$, 11.7 mM D-glucose, 1.18 mM $MgSO_4 \cdot 7H_2O$, 1.18 mM KH_2PO_4, 4.69 mM KCl, 118 mM NaCl, 1.29 mM $CaCl_2 \cdot 2H_2O$, and 0.01% (w/v) BSA, pH 7.4]. Cells were then mounted onto the stage of an Olympus IX50 inverted microscope and maintained at 37°C using a Peltier heated coverslip holder. Confocal imaging of the eGFP-tagged biosensors was monitored using either an Olympus FV500 or an Ultra*VIEW* confocal microscope (PerkinElmer Life and Analytical Sciences, Boston, MA) as described previously (Nash et al., 2002; Witherow et al., 2003). In brief, eGFP was excited using the 488 nm laser line, and the emitted fluorescence was captured at wavelengths >505 nm, with images collected at 1-s intervals. Analysis was carried out using software supplied by the confocal manufacturer (Olympus Fluoview or PerkinElmer Imaging Suite), with raw fluorescence data exported to Microsoft Excel and expressed as F/F_o (eGFP fluorescence/basal eGFP fluorescence) for each cell. For Ca^{2+} imaging, cells were loaded with fluo-3 in KHB by incubation with fluo-3-acetoxymethyl ester (2 μM prepared in anhydrous dimethyl sulfoxide; TEF Laboratories, Austin, TX) for 45 min at 20°C followed by a further 45-min incubation in KHB to allow de-esterification of the indicator. Measurement of the intracellular Ca^{2+} concentration ($[Ca^{2+}]_i$) was performed using either an Olympus FV500 or a PerkinElmer Ultra*VIEW* confocal microscope with images collected every second. Analysis and data processing was performed as described previously for eGFP. For imaging experiments, data are reported as the average ± S.E.M. for *n* cells from at least three individual coverslips.

Measurement of Total PLC Activity. Agonist-induced accumulation of ^{3}H-labeled mono- and polyphosphates of inositol ($[^3H]InsP_x$) was determined in cells prelabeled with [*myo*-^{3}H]inositol in which inositol monophosphatase activity was blocked with Li^+. Cells were prelabeled with 3 μCi/ml of [*myo*-^{3}H]inositol (76 Ci/mmol) for 48 h in 24-well multidishes to ensure equilibrium labeling. On the day of experiments, the media was removed and replaced with 250 μl of KHB supplemented with 10 mM LiCl. After a 10-min incubation, cells were stimulated by the addition of 250 μl of KHB containing Li^+ and agonist at twice the required concentration. Stimulations were carried out in triplicate; after a 20-min incubation, reactions were terminated by the addition of an equal volume of 1 M trichloroacetic acid. $[^3H]InsP_x$ were extracted and separated by anion exchange chromatography exactly as described previously (Wheldon et al., 2001). Experimental data are reported as the mean ±/+ S.E.M. of *n* experiments.

Data Analysis. In all cases, data are reported as the mean ±/+ S.E.M. for *n* experiments. For imaging experiments, *n* refers to the number of cells for each condition taken from *n* different coverslips. For experiments measuring total PLC activity, *n* refers to the number of different accumulations. Statistical analysis was carried out using one-way ANOVA; where P was < 0.05, it was followed by Dunnett's range test. In all cases, * represents $P < 0.05$; **, $P < 0.01$; and ***, $P < 0.001$ by the range test.

Results

Transient Expression of *myc*-Tagged rgs Proteins. To determine the expression of RGS proteins and allow expression at equivalent levels where required, a C-terminal *myc*-epitope tag was incorporated into the DNA sequence encoding RGS2, RGS3, and RGS4. Expression of the RGS*myc* fusion proteins allowed subsequent immunoblotting of the *myc*-epitope tag (and hence RGS protein) with an anti-*myc* antibody. In HEK293/M_3 cells transiently transfected with plasmid DNAs, the anti-*myc* antibody recognized proteins at the expected molecular masses for RGS2*myc* (~28 kDa), RGS3*myc* (~80 kDa), and RGS4*myc* (~28 kDa) (Fig. 1). After transfection of either HEK293/M_3 cells (Fig. 1) or HEK293/WT cells (data not shown) with identical amounts of plasmid DNAs encoding either RGS2*myc*, RGS3*myc*, or RGS4*myc*, the expression level of RGS3*myc* (and the LacZ-*myc* control) was consistently 2- to 3-fold greater than either RGS2*myc* or RGS4*myc*.

Subcellular Localization of RGS Proteins. To evaluate the subcellular distribution of expressed recombinant RGS proteins, HEK293/M_3 cells were transiently transfected with the RGS*myc* DNA constructs, and protein localization was determined by immunocytochemistry using an anti-*myc* primary antibody and a FITC-labeled secondary antibody. The distribution of fluorescence indicated that RGS2*myc* was expressed at high levels in the nucleus compared with the cytoplasm (Fig. 2a). In contrast, both RGS3*myc* and RGS4*myc* were predominantly cytosolic (Fig. 2, b and c). Immunocytochemistry of untransfected cells or addition of the secondary antibody only to transfected cells revealed no cellular staining under conditions identical to those used above (data not shown).

Single-Cell Imaging of Ins(1,4,5)P_3 Generation. Protein-based biosensors have recently been developed that can detect the generation of either Ins(1,4,5)P_3 (eGFP-$PH_{PLC\delta1}$) or diacylglycerol (eGFP-PKCγC1$_2$) in real time at the single-cell level. In this study, we first used eGFP-$PH_{PLC\delta1}$ to determine the ability of either untagged or *myc*-tagged RGS2,

RGS3, and RGS4 to inhibit muscarinic receptor-mediated generation of Ins(1,4,5)P_3 in HEK293/M_3 cells. In cells transiently transfected with the eGFP-$PH_{PLC\delta1}$ biosensor alone, challenge with 100 μM methacholine resulted in a rapid and robust translocation of eGFP fluorescence from the membrane to the cytoplasm in all cells examined [e.g., Fig. 3a(i)]. Determination of the cytosolic fluorescence indicated a rapid, marked, and sustained increase in the level of cytosolic fluorescence (Fig. 3b) reflective of agonist-mediated Ins(1,4,5)P_3 accumulation (Nash et al., 2001, 2002). In contrast, in cells cotransfected with both the eGFP-$PH_{PLC\delta1}$ biosensor and RGS3*myc*, 100 μM methacholine had no effect on the plasma membrane localization of eGFP fluorescence (Fig. 3, a(ii) and b) demonstrating a marked inhibition of muscarinic receptor-mediated Ins(1,4,5)P_3 accumulation. Quantification of the maximal increase in cytosolic fluorescence in the 60 s after agonist addition provides an index of the maximal extent of Ins(1,4,5)P_3 accumulation. Data collected over a series of experiments demonstrated that expression of untagged or *myc*-tagged versions of either RGS2 or RGS3 markedly inhibited Ins(1,4,5)P_3 responses to maximal activation of muscarinic receptors in HEK293/M_3 cells (Fig. 3c). In contrast, expression of either RGS4 or RGS4*myc* did not affect the magnitude of Ins(1,4,5)P_3 responses to 100 μM methacholine (Fig. 3c).

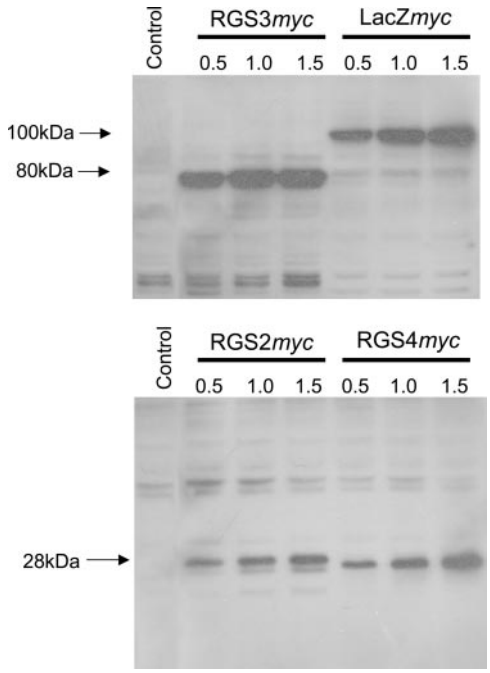

Fig. 1. Transient overexpression of *myc*-tagged RGS proteins. Western blot of HEK293/M_3 cell lysates (30 μg of protein/lane), showing the transient over-expression of *myc*-tagged RGS proteins. The number above each lane corresponds to the amount of RGS*myc* DNA transfected. Control lanes are samples from untransfected HEK293/M_3 cells. Blots are representative of cell lysates obtained from at least three different transient transfections.

The Expression Level of RGS3*myc* Determines the Extent of Inhibition of Agonist-Mediated Ins(1,4,5)P_3 Generation. In the experiments described above, the transient transfection of HEK293/M_3 cells with matched levels of DNA for the different RGS*myc* constructs resulted in a higher level of expression of RGS3*myc* compared with either RGS2*myc* or RGS4*myc* (Fig. 1). In additional experiments, we therefore reduced the amount of RGS3*myc* plasmid DNA used in the transfection in an effort to lower the expression level of RGS3*myc* to levels equivalent with RGS2*myc* and RGS4*myc*. Western blotting of cell lysates after transfection demonstrated that reducing the amount of RGS3*myc* plasmid DNA resulted in a reduced level of RGS3*myc* expression (Fig. 4a). Densitometric analysis of Western blots indicated that HEK293/M_3 cells transfected with 0.5 μg/well of RGS3*myc* plasmid DNA expressed levels of RGS*myc* protein approximately equivalent to those expressed by cells transfected with 1.5 μg/well of either RGS2*myc* or RGS4*myc* DNA (data not shown). Functional experiments with eGFP-$PH_{PLC\delta1}$ demonstrated that with increasing amounts of transfected RGS3*myc* plasmid DNA, the degree of inhibition of Ins(1,4,5)P_3 production increased (Fig. 4b). At a concentration of 0.5 μg/well of RGS3*myc* plasmid DNA, there was partial (~50%) inhibition of Ins(1,4,5)P_3 accumulation in response to a maximal concentration of methacholine (100 μM) but a complete inhibition of signaling in response to a submaximal (~EC_{50}) concentration of methacholine (1 μM) (Fig. 4b). One consideration is that at lower amounts of RGS3*myc* plasmid DNA, there were fewer cells expressing both the eGFP-$PH_{PLC\delta1}$ biosensor and RGS3*myc*. However, in similar studies in which we varied the amount of RGS3*myc* plasmid DNA, the proportion of cells expressing RGS3*myc*, as assessed by immunocytochemistry, were similar (data not shown). Furthermore, in the functional studies using the eGFP-$PH_{PLC\delta1}$ biosensor, there was no evidence for the emergence of two distinct populations of cells (i.e., those in which signaling was inhibited and those in which it was not) (Fig. 4c). Concentration-response curves for methacholine-mediated membrane to cytosol translocation of the eGFP-$PH_{PLC\delta1}$ biosensor demonstrated that the expression of either LacZ*myc* or RGS4*myc* (1.5 μg of plasmid DNA/well) did not affect agonist-mediated Ins(1,4,5)P_3 accumulation (Fig. 5). This was reflected in E_{max} values and pEC_{50} values that were not significantly different from those in cells transfected with the biosensor alone [pEC_{50} values: control, 6.4 $\pm$ 0.1 (n = 3); LacZ*myc*, 6.1 $\pm$ 0.1 (n = 3); RGS4*myc*, 6.3 $\pm$ 0.3 (n = 3)]. The expression of RGS2*myc* and RGS3*myc* (1.5 μg of plasmid DNA/well), however, did reduce the E_{max} of metha-

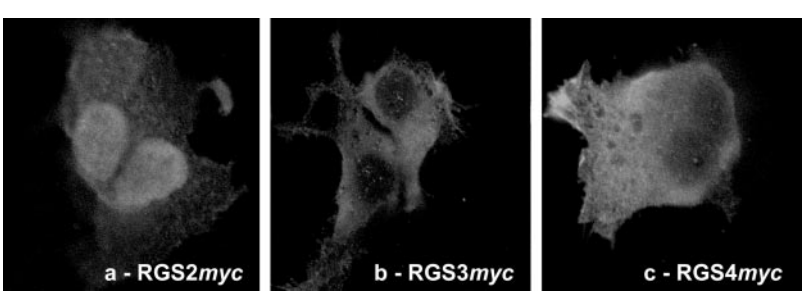

Fig. 2. Subcellular localization of RGS proteins. Immunolocalization of RGS2*myc*, RGS3*myc*, or RGS4*myc* transiently overexpressed in HEK293/M_3 cells. The *myc*-tag was detected using an anti-*myc* antibody, which was subsequently labeled with a FITC-conjugated secondary antibody. Images are typical of at least three different transient transfections and immunolabeling experiments.

choline-mediated Ins(1,4,5)P_3 accumulation (Fig. 5). The extent of the inhibitory effect of RGS3*myc* was dependent upon the level of expression. Thus, when the expression levels of RGS2*myc* and RGS3*myc* were matched (by reducing the RGS3*myc* plasmid DNA to 0.5 μg of plasmid DNA/well), the extent of inhibition by RGS2*myc* and RGS3*myc* were approx-

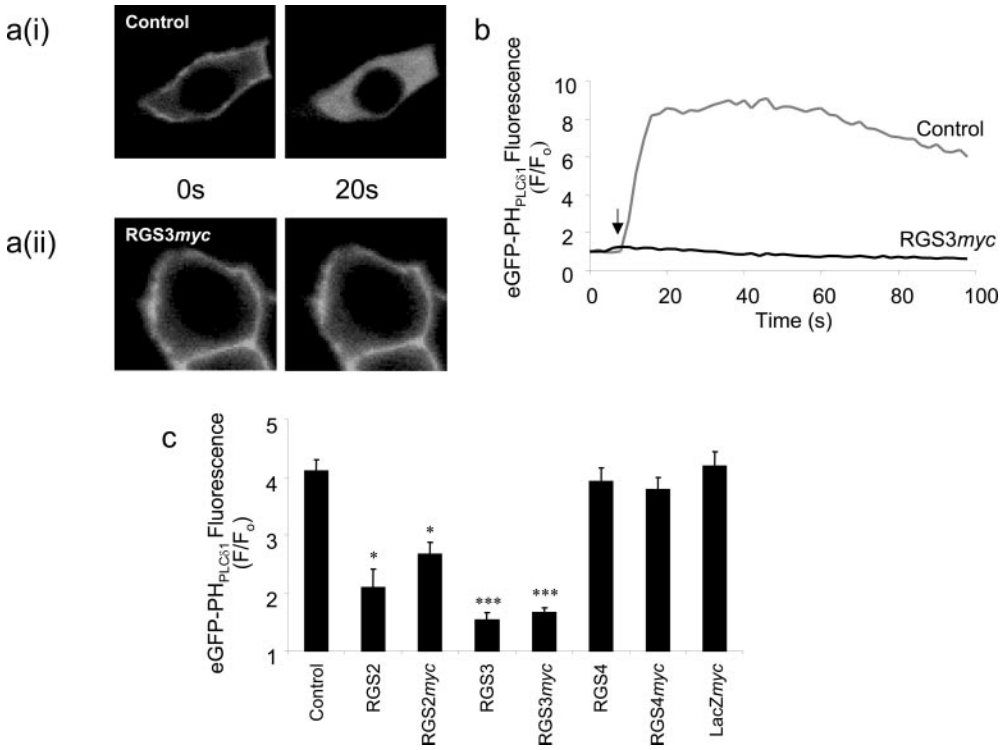

Fig. 3. Single-cell imaging of Ins(1,4,5)P_3 production. a(i), typical single-cell confocal images of HEK293/M_3 cells transiently transfected with the Ins(1,4,5)P_3 biosensor, eGFP-$PH_{PLC\delta1}$. Under resting conditions (0 s), the eGFP-tagged biosensor is localized to the plasma membrane, but upon agonist stimulation (100 μM methacholine), eGFP-$PH_{PLC\delta1}$ translocates to the cytosol (20 s) corresponding to the production of Ins(1,4,5)P_3. a(ii), in HEK293/M_3 cells transiently cotransfected with eGFP-$PH_{PLC\delta1}$ and RGS3*myc*, the translocation of the eGFP-tagged biosensor is reduced, corresponding to an inhibition of Ins(1,4,5)P_3 production. b, sample traces of the change in cytoplasmic eGFP fluorescence with time upon muscarinic M_3 receptor stimulation in HEK293/M_3 cells. Traces represent HEK293/M_3 cells transiently transfected with either eGFP-$PH_{PLC\delta1}$ alone (upper trace) or cells transiently cotansfected with both eGFP-$PH_{PLC\delta1}$ and RGS3*myc* (lower trace). The arrow represents the time point for the addition of methacholine (100 μM). c, summary of data from the type of experiments described above. Data represent the mean peak increase in cytoplasmic eGFP fluorescence + S.E.M. for 20 to 40 cells from at least four different coverslips. Statistical comparisons were by one-way ANOVA with Dunnett's range test; *, $P < 0.05$; ***, $P < 0.001$ versus control.

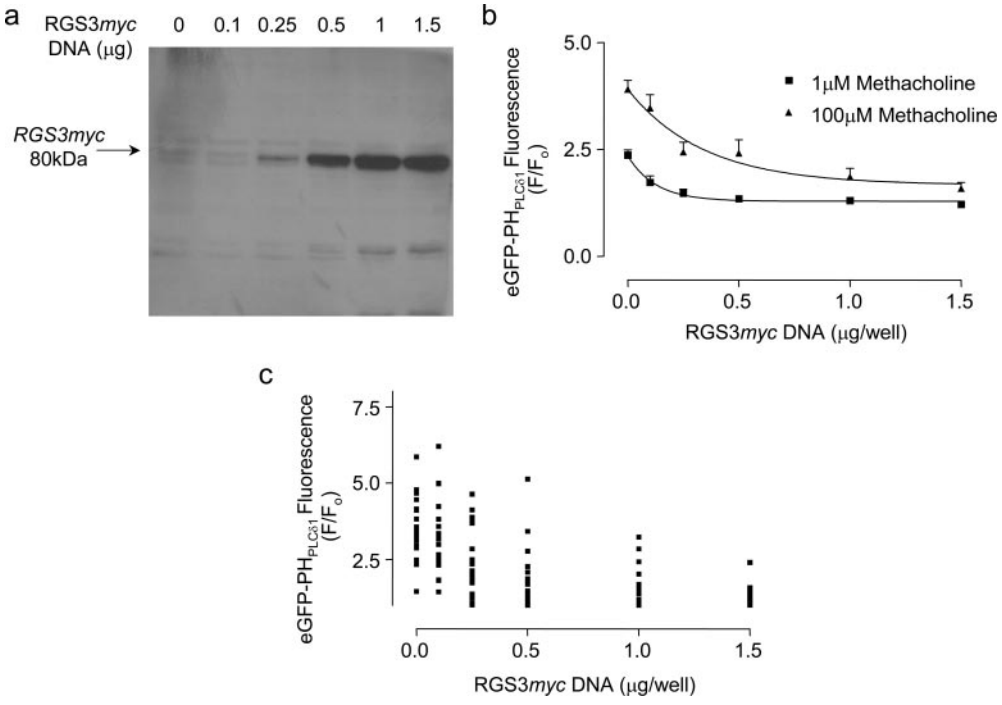

Fig. 4. Decreasing RGS3*myc* expression relieves inhibition of Ins(1,4,5)P_3 generation. a, immunoblot showing increasing transient expression of RGS3*myc* in HEK293/M_3 cells with increasing amounts of RGS3*myc* DNA. The blot is representative of blots from three different transient transfections. b, increasing the level of RGS3*myc* expression in HEK293/M_3 cells leads to a decreased level of Ins(1,4,5)P_3 production. Data represent the mean change in peak cytoplasmic eGFP fluorescence + S.E.M. for 20 to 30 cells from at least three different coverslips. c, scatter plot of data from b (100 μM methacholine).

imately equivalent (Fig. 5). Although both RGS2*myc* and RGS3*myc* reduced the E_{max} of responses, agonist potency was unaffected compared with controls [pEC_{50} values: RGS2*myc*, 6.4 ± 0.1 (n = 3); RGS3*myc* 0.5 μg of plasmid DNA/well, 6.3 ± 0.3 (n = 3); RGS3*myc* 1.5 μg of plasmid DNA/well, 5.8 ± 0.1 (n = 3)]. In addition to inhibiting the magnitude of muscarinic receptor-mediated Ins(1,4,5)P_3 responses, RGS2*myc* and RGS3*myc* inhibited the rate of Ins(1,4,5)P_3 generation at both submaximal (1 μM) and maximal (100 μM) concentrations of methacholine, as implied by reductions in the rate of change of the cytosolic fluorescence (Table 1). Although RGS4*myc* did not influence the maximal change in cytosolic fluorescence at any concentration of methacholine, it did reduce the rate of change at both submaximal and maximal concentrations of methacholine (Table 1).

Single-Cell Imaging of Diacylglycerol Production. To assess the potential impact of the RGS proteins on the other limb of the signaling pathway resulting from PLC-mediated hydrolysis of phosphatidylinositol 4,5-bisphosphate, and to confirm that the effects were not specific to the eGFP-$PH_{PLC\delta1}$ biosensor, we next assessed the effects of RGS*myc* proteins on muscarinic receptor-mediated diacylglycerol production using the eGFP-PKCγC1$_2$ biosensor. Transient transfection of eGFP-PKCγC1$_2$ in HEK293/M_3 cells resulted in the expression of cytosolic fluorescence that translocated to the plasma membrane upon addition of 100 μM methacholine in all cells (Fig. 6a(i)). Determination of the cytosolic fluorescence showed that the agonist-mediated loss of cytosolic fluorescence occurred immediately on agonist addition, was maximal by approximately 20 s but largely restored over the subsequent 140 s despite the continued presence of methacholine (Fig. 6b). The coexpression of RGS3*myc* with the eGFP-PKCγC1$_2$ biosensor abolished the cytosol to membrane translocation of eGFP fluorescence upon addition of 100 μM methacholine (Fig. 6, a(ii) and b), indicating marked inhibition of diacylglycerol accumulation. The expression of RGS2*myc* also significantly inhibited translocation of eGFP fluorescence in response to 100 μM methacholine (Fig. 6c). In contrast, expression of RGS4*myc* did not influence the response (Fig. 6c).

Generation of HEK293 Cell Lines with Stable Expression of RGS*myc* Proteins. To overcome the limitations of transient transfection protocols (e.g., potentially variable transfection efficiency and a limited ability to carry out population-based measurements), we generated HEK293 cell lines with stable expression of RGS2*myc*, RGS3*myc*, or RGS4*myc*. Transfection of HEK293/WT cells with RGS*myc* plasmid DNAs resulted in the generation of cell lines from which single clones of cells expressing either RGS2*myc* (HEK293/RGS2*myc*), RGS3*myc* (HEK293/RGS3*myc*), or RGS4*myc* (HEK293/RGS4*myc*) were selected on the basis of similar expression levels of the *myc*-tagged proteins (Fig. 7a). HEK cells endogenously express the muscarinic M_3 receptor (Ancellin et al., 1999). After selection, the expression of endogenous muscarinic receptors was assessed using [*N*-methyl-^{3}H]scopolamine methyl chloride binding to intact cells. Each of the cell lines had expression levels similar to HEK293/WT (~40 fmol/mg of total cell protein; data not shown). Furthermore, levels of G$\alpha_{q/11}$ were similar as assessed by immunoblotting with a previously characterized antibody (Mitchell et al., 1991) (data not shown). Immunocytochemistry demonstrated that the subcellular distribution of the stably expressed RGS*myc* proteins was identical to their distribution when expressed transiently (see Fig. 2).

Receptor- and AlF_4^--Mediated PLC Activity in Cell Lines That Have Stable Expression of RGS*myc* Proteins. Transfection of the eGFP-$PH_{PLC\delta1}$ biosensor plasmid DNA into HEK/WT cells results in the expression of membrane-localized fluorescence identical to that seen in HEK293/M_3 cells. However, activation of the endogenously expressed muscarinic receptors with 100 μM methacholine caused little or no membrane-to-cytosol translocation in these cells. This is consistent with a lack of methacholine-mediated accumulation of Ins(1,4,5)P_3 mass in populations of these cells (data not shown) measured using a well characterized radioreceptor assay (Willars and Nahorski, 1995). In contrast, 100 μM methacholine evoked an accumulation of [^{3}H]InsP_x against a Li^+-block of inositol monophosphatase in these cells. Accumulation of [^{3}H]InsP_x in such experiments is independent of the metabolism of Ins(1,4,5)P_3 and reflects total PLC activity (Willars et al., 1998a,b). A 20-min stimulation of HEK293/WT cells with either 1 or 100 μM methacholine resulted in a 2.5 ± 0.1 (n = 5) and 8.1 ± 0.5 (n = 5) fold-over basal accumulation of [^{3}H]InsP_x, respectively (Fig. 7b). The extent of accumulation was similar in cells express-

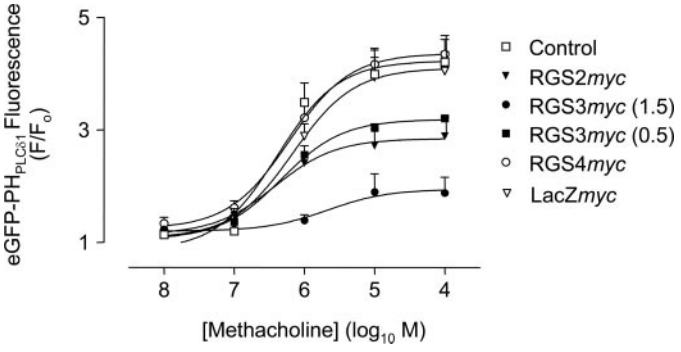

Fig. 5. The effect of RGS*myc* protein expression on the concentration-dependence of methacholine-mediated Ins(1,4,5)P_3 generation. Concentration-response curves (0.01–100 μM methacholine) for single-cell Ins(1,4,5)P_3 production in control HEK293/M_3 cells and HEK293/M_3 cells transiently transfected with either RGS2*myc*, RGS3*myc*, RGS4*myc*, or a LacZ*myc* control vector. Data represent the mean change in cytoplasmic eGFP fluorescence + S.E.M. for 20 to 30 cells from at least three different coverslips.

TABLE 1

Kinetics of increases in cytosolic fluorescence in response to agonist stimulation in HEK/M_3 cells expressing the Ins(1,4,5)P_3 biosensor, eGFP-$PH_{PLC\delta1}$

Cells transiently transfected with eGFP-$PH_{PLC\delta1}$ either alone (control) or with an RGS*myc* construct or with a control vector (LacZ*myc*), were imaged by confocal microscopy and challenged with either 1 or 100 μM methacholine. Data are presented as 1/rise time (s^{-1}), where the rise time was taken to be the time to reach a peak response from the initial point of inflection. Data are mean ± S.E.M., with the number of cells analyzed in parentheses. Statistical comparisons were by one-way ANOVA with Dunnett's range test.

	Methacholine			
	1 μM		100 μM	
Control	0.08 ± 0.01	(n = 15)	0.15 ± 0.01	(n = 17)
RGS2*myc*	0.06 ± 0.004*	(n = 8)	0.09 ± 0.01**	(n = 15)
RGS3*myc* (0.5 μg)	0.05 ± 0.01*	(n = 10)	0.10 ± 0.01**	(n = 12)
RGS3*myc* (1.5 μg)	N.D.		0.08 ± 0.01**	(n = 4)
RGS4*myc*	0.04 ± 0.002***	(n = 13)	0.10 ± 0.01***	(n = 19)
LacZ*myc*	0.08 ± 0.01	(n = 14)	0.15 ± 0.01	(n = 17)

* $P < 0.05$; ** $P < 0.01$; *** $P < 0.001$ versus appropriate control; N.D., not determined.

ing RGS4*myc* but significantly reduced in cells expressing RGS2*myc* and essentially abolished in cells expressing RGS3*myc* (Fig. 7b). The direct stimulation of G-proteins with aluminum fluoride (AlF_4^-) also caused a 3.1 ± 0.1-fold ($n = 3$) increase over basal accumulation of [^{3}H]InsP_x over a 30-min period (Fig. 7b). This AlF_4^--mediated accumulation of [^{3}H]InsP_x, however, was unaffected by the expression of RGS2*myc*, RGS3*myc*, or RGS4*myc* in the clonal cell lines (Fig. 7b).

The Effect of RGS Proteins on the Amplitude, Kinetics, and Pattern of Receptor-Mediated Ca^{2+} Signals. Single-cell imaging of intracellular Ca^{2+} signaling in HEK293/WT cells revealed that low concentrations of methacholine (1 μM) caused repetitive whole-cell Ca^{2+} oscillations that subsided gradually with time and in which the $[Ca^{2+}]_i$ returned to approximately basal levels between oscillations (Fig. 8a(i)). In cells expressing either RGS2*myc*, RGS3*myc*, or RGS4*myc*, there were significant reductions in both the magnitude of the initial Ca^{2+} response (Figs. 8, a(i–iv), and 9a) and the rise-time of the initial peak (Fig. 9b) in response to this submaximal concentration of methacholine (1 μM). Expression of the RGS proteins was also associated with a dampening of the magnitude and frequency of subsequent oscillations (Figs. 8, a(i–iv) and 9c). A higher concentration of methacholine (100 μM) resulted in more robust Ca^{2+} signaling in HEK293/WT cells (Fig. 8, compare a(i) and b(i)). The majority of cells responded with a rapid peak of Ca^{2+} elevation followed by a more sustained phase, although some cells oscillated around this elevated level. In cells expressing either RGS2*myc* or RGS3*myc*, there were significant reductions in the amplitude and rise-time of the initial peak response (Fig. 9, a and b). However, expression of these RGS proteins resulted in an increase in oscillatory behavior (Figs. 8, b(i–iii), and 9c). RGS4*myc* affected neither the amplitude nor the rise time of the initial peak Ca^{2+} response to 100 μM methacholine (Figs. 8, b(i) and b(iv), and 9, a and b), although a slight increase in oscillatory behavior was observed (Fig. 8, b(i) and b(iv)).

RGS Proteins Inhibit Ca^{2+} Signals Mediated by the Endogenous $G\alpha_{q/11}$-Coupled $P2Y_2$ Receptor. There is some evidence that RGS proteins are selective among different receptor types that couple to $G\alpha_{q/11}$ (Zeng et al., 1998; Xu et al., 1999), and recent evidence has suggested that this may be a consequence of interactions between the GPCR and RGS protein (Bernstein et al., 2004). HEK293 cells also express endogenous $P2Y_2$ nucleotide receptors that couple to $G\alpha_{q/11}$ (Werry et al., 2002), and we therefore carried out a preliminary investigation of the impact of RGS protein expression on signaling by these receptors. Stimulation of $P2Y_2$ nucleotide receptors with a maximal concentration of UTP resulted in $[Ca^{2+}]_i$ responses similar to those seen with 100 μM methacholine (data not shown). UTP-mediated Ca^{2+} signaling was also inhibited by expression of RGS2*myc* and even more so by RGS3*myc* as judged by reductions in the amplitude of the initial peak response (Fig. 9d). However, RGS4*myc* had no effect on the Ca^{2+} responses to this maximal concentration of UTP (Fig. 9d).

The Effect of RGS Proteins on AlF_4^--Medicated CA^{2+} Signaling. After addition of AlF_4^- to HEK293/WT cells, there

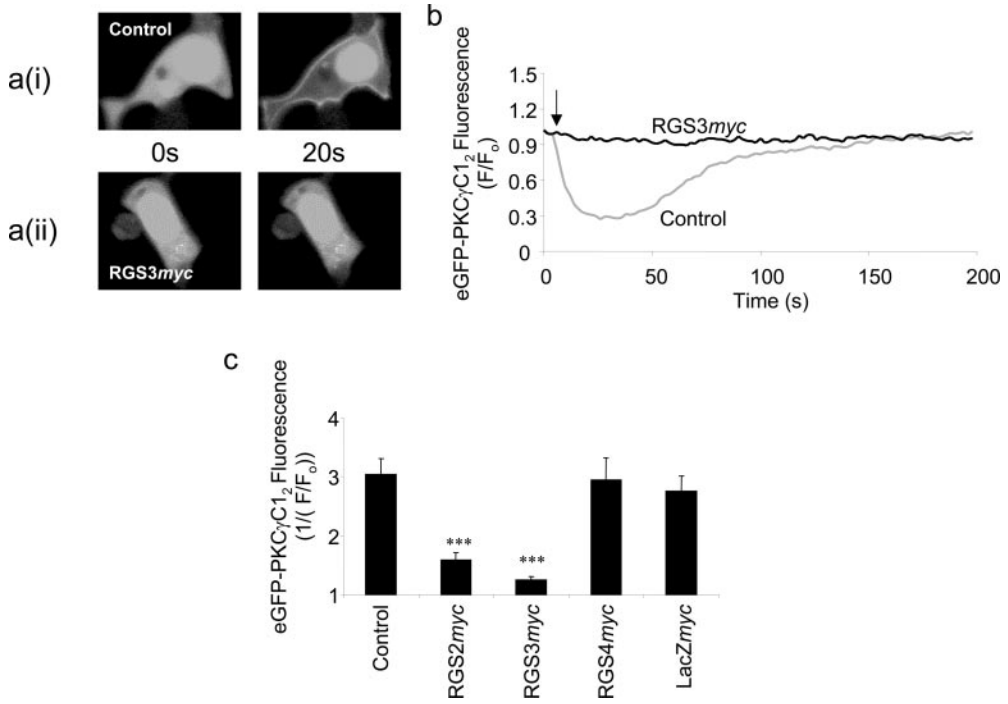

Fig. 6. Single-cell imaging of diacylglycerol production. a(i), typical single-cell confocal images of HEK293/M_3 cells transiently transfected with the diacylglycerol biosensor eGFP-PKCγC1$_2$. Under resting conditions (0 s), the eGFP-tagged biosensor is localized homogeneously across the cell cytoplasm and nucleus, but upon agonist stimulation (100 μM methacholine), the eGFP translocates to the plasma membrane (20 s) corresponding to the production of diacylglycerol. a(ii), in HEK293/M_3 cells transiently cotransfected with both eGFP-PKCγC1$_2$ and RGS3*myc*, the translocation of the eGFP-tagged biosensor is reduced, corresponding to an inhibition of diacylglycerol production. b, sample traces of the change in cytoplasmic eGFP fluorescence with time upon muscarinic M_3 receptor stimulation in HEK293/M_3 cells. Traces represent HEK293/M_3 cells transiently transfected with eGFP-PKCγC1$_2$ alone (lower trace) and cells transiently cotransfected with both eGFP-PKCγC1$_2$ and RGS3*myc* (upper trace). The arrow represents the time point for the addition of methacholine (100 μM). c, summary of data from the type of experiments described above. Data represent the mean + S.E.M. for 13 to 30 cells from at least three different coverslips. Statistical comparisons were by one-way ANOVA with Dunnett's range test; ***, $P < 0.001$ versus control.

was a lag period of 105 ± 8 s (n = 15) before the appearance of baseline Ca^{2+} oscillations (Fig. 10a) that were similar to those evoked by a low concentration (1 μM) of methacholine (Fig. 8a(i)). The amplitude of the initial Ca^{2+} response to AlF_4^- was not significantly affected by the expression of the RGS*myc* proteins (Fig. 10, b and c). Furthermore, oscillation frequency was not affected [HEK293/WT, 1.69 ± 0.09 oscillations in 100 s (n = 48); RGS2*myc*, 1.67 ± 0.14 oscillations in 100 s (n = 30); RGS3*myc*, 1.74 ± 0.07 oscillations in 100 s (n = 38); and RGS4*myc*, 1.54 ± 0.08 oscillations in 100 s (n = 48)]. However, the lag phase between the addition of AlF_4^- and the first Ca^{2+} response was significantly longer in the RGS*myc*-expressing cell lines [RGS2*myc*, 173 ± 5 s (n = 27); RGS3*myc*, 218 ± 8 s (n = 15); RGS4*myc*, 177 ± 6 s (n = 44); all $P < 0.001$ versus HEK293/WT cells].

The Effect of RGS Proteins on PLC Signaling Mediated by Constitutively Active $G\alpha_q$. Next, we sought to establish the impact of RGS*myc* protein expression on signaling mediated by a CA-$G\alpha_q$ (Q209L) that is insensitive to the GTPase activity of RGS proteins (Heximer et al., 2001). In HEK293/WT cells transiently transfected with CA-$G\alpha_q$ (0.25 μg/well of a 24-well multidish), the addition of 10 mM Li^+ to block inositol monophosphatase activity for 20 min resulted in a 3.6 ± 0.4-fold (n = 3) increase in $[^3H]InsP_x$ accumulation compared with control, untransfected cells. Addition of Li^+ to cells with transient expression of CA-$G\alpha_q$ and stable expression of one of the RGS*myc* proteins also resulted in the accumulation of $[^3H]InsP_x$ (Fig. 11). The accumulation

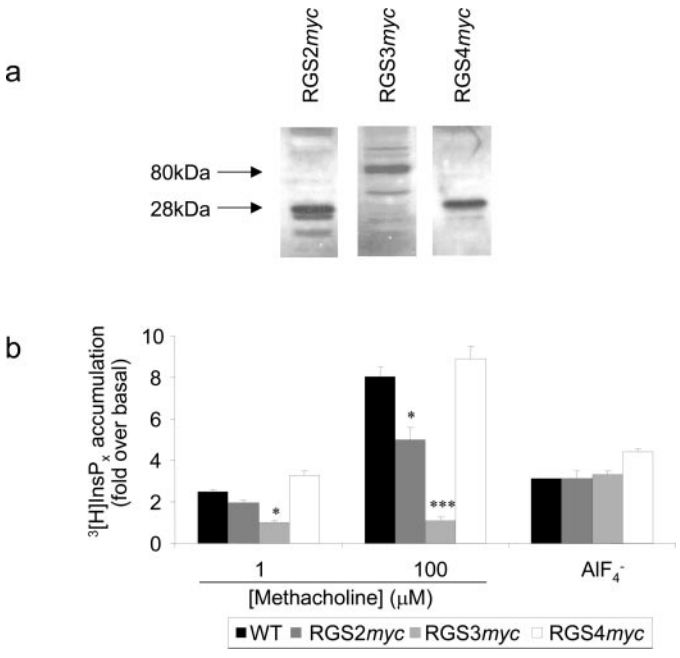

Fig. 7. Generation of stable RGS*myc* expression in HEK293 cells. a, Western blot of whole cell lysates (20 μg of protein/lane) from HEK293 cells illustrating stable expression of either RGS2*myc*, RGS3*myc*, or RGS4*myc*. The blot is representative of at least three different blots for each cell line. b, total inositol phosphate ($[^3H]InsP_x$) accumulation under a Li^+ block in HEK293/WT, HEK293/RGS2*myc*, HEK293/RGS3*myc*, and HEK293/RGS4*myc* cells. Data are shown for stimulation of the endogenous muscarinic M_3 receptor with either 1 or 100 μM methacholine and also for receptor-independent activation of G-proteins with AlF_4^- (50 mM NaF; 50 μM $AlCl_3$). Data are represented as the mean + S.E.M. for at least three separate accumulations. Statistical comparisons were by one-way ANOVA with Dunnett's range test; *, $P < 0.05$; ***, $P < 0.001$ versus control.

of $[^3H]InsP_x$ was significantly greater in cell lines expressing either RGS2*myc* or RGS3*myc* compared with either HEK293/WT cells or cells expressing RGS4*myc* (Fig. 11).

Discussion

In this study, we compared the abilities of members of the B/R4 family of RGS proteins to inhibit Ca^{2+} and phosphoinositide signaling by $G\alpha_{q/11}$-coupled muscarinic receptors. We selected RGS4 as the prototypical member of the B/R4 family along with RGS2, given its high specificity for $G\alpha_q$ (Heximer et al., 1997). We also selected RGS3, in that although its RGS domain has high homology with other family members, it is atypical in that it has a large N terminus of unknown function (Hollinger and Hepler, 2002). Previous studies suggest that each of these RGS proteins influence $G\alpha_{q/11}$ signaling (Hollinger and Hepler, 2002) and that RGS2 and RGS4 have different inhibitory activities (Heximer et al., 1997).

In the present study, we used single-cell imaging techniques to enable a more precise understanding of the influence of the RGS proteins on the magnitude and kinetics of signaling. In particular, this has allowed the determination of the effects of RGS proteins on PLC-mediated signaling in the seconds immediately after receptor activation. This is of considerable importance given that the vast majority of PLC-coupled GPCRs undergo either full or partial desensitization within seconds of agonist addition, most probably through receptor phosphorylation. The muscarinic M_3 receptor is a well-studied example of such a receptor; it has an initial, rapidly desensitized component of signaling followed by a sustained, desensitization-resistant phase. Many previous studies examining the effects of RGS proteins on PLC have determined inositol phosphate accumulation against a Li^+-block of inositol monophosphatase over many minutes. This will neither reflect the levels of the second messenger, $Ins(1,4,5)P_3$, nor reflect the impact of RGS proteins on the immediate, probably physiologically relevant phase of receptor activation. Furthermore, the initial and sustained phases of receptor signaling can be driven with different agonist potencies (Willars and Nahorski, 1995) and are clearly subject to different regulatory features.

RGS2 and RGS3 inhibited both the magnitude and rate of the immediate, agonist-induced $Ins(1,4,5)P_3$ generation in single cells during maximal receptor activation as assessed using the eGFP-$PH_{PLC\delta1}$ biosensor. In contrast, RGS4 had no effect on the magnitude but more subtly reduced the rate of generation. It is noteworthy that the effects of the *myc*-tagged and untagged RGS proteins were identical. This is consistent with other studies in which RGS2 and RGS4 have been similarly tagged without consequence (Srinivasa et al., 1998; Heximer et al., 1999).

Although muscarinic receptor-mediated $Ins(1,4,5)P_3$ accumulation was inhibited in the order RGS3 > RGS2 > RGS4, immunoblotting showed RGS3*myc* expression was greater than either RGS2*myc* or RGS4*myc*. It is interesting that untagged versions showed levels of inhibition similar to those of their *myc*-tagged counterparts, suggesting similar differences in expression levels and that these are a feature of the RGS proteins. This could reflect interactions with other proteins, which can result in stabilization of the RGS protein (Witherow et al., 2000). Reducing the amount of transfected DNA reduced both the expression of RGS3*myc* and the inhi-

bition of receptor-mediated Ins(1,4,5)P_3 generation. At approximately equivalent expression levels, inhibition by RGS3*myc* was more consistent with that of RGS2*myc*. Despite effects of RGS2*myc* and RGS3*myc* on Ins(1,4,5)P_3 generation, agonist potency was unaffected.

We also used the eGFP-PKCγC1$_2$ biosensor to examine diacylglycerol formation, which is complimentary to Ins(1,4,5)P_3 but has distinct signaling consequences. When expressed at similar levels, RGS2*myc* and RGS3*myc* but not RGS4*myc* inhibited diacylglycerol formation as assessed by reduced cytosol to membrane translocation of eGFP-PKCγC1$_2$.

To increase the utility of our model, we generated stable cell lines from HEK293/WT cells that expressed the RGS*myc* proteins at similar levels. RGS2*myc* and RGS3*myc* reduced both the amplitude and kinetics of single-cell Ca^{2+} events at maximal and submaximal agonist concentrations. In contrast, inhibitory effects of RGS4*myc* were only apparent at submaximal agonist concentrations. The RGS proteins also influenced the patterns of Ca^{2+} signaling. At low agonist concentrations that produced oscillatory Ca^{2+} patterns in HEK293/WT cells, the RGS*myc* proteins dampened both the amplitude and frequency of oscillations. In contrast, at high agonist concentrations that produced essentially peak and sustained Ca^{2+} responses in HEK293/WT cells, RGS*myc* expression promoted oscillatory Ca^{2+} signaling. The pattern of Ca^{2+} signaling is key in defining the cellular responses to agonist stimulation, and the demonstration that RGS proteins can influence the pattern as well as the extent of Ca^{2+} signaling has important physiological implications. The precise mechanisms underlying oscillatory Ca^{2+} signaling are unclear. Low levels of Ins(1,4,5)P_3 may sensitize its receptor to Ca^{2+}-induced Ca^{2+} release and promote regenerative Ca^{2+} oscillations, whereas at higher levels, a dynamic (oscillatory) uncoupling of the GPCR signaling complex (e.g., receptor phosphorylation/dephosphorylation) may regulate oscillations (Nash et al., 2002). At still higher levels of Ins(1,4,5)P_3, its receptors may saturate, causing peak and plateau Ca^{2+} responses. In our studies, reduced Ins(1,4,5)P_3 could account for RGS protein effects at both low and high agonist concentrations. We cannot exclude the possibility, however, that oscillatory changes in G$\alpha_{q/11}$ activation caused by cycles of activation and inactivation of RGS proteins cause oscillatory Ca^{2+} signaling, as suggested recently (Luo et al., 2001).

The greater inhibitory activity of RGS2 compared with RGS4 is consistent with an earlier cellular study that examined inositol phosphate accumulation (Heximer et al., 1999) but contrasts with that observed in vitro (RGS2 > RGS3 = RGS4) (Heximer et al., 1997; Scheschonka et al., 2000). This suggests that other factors may determine RGS protein spec-

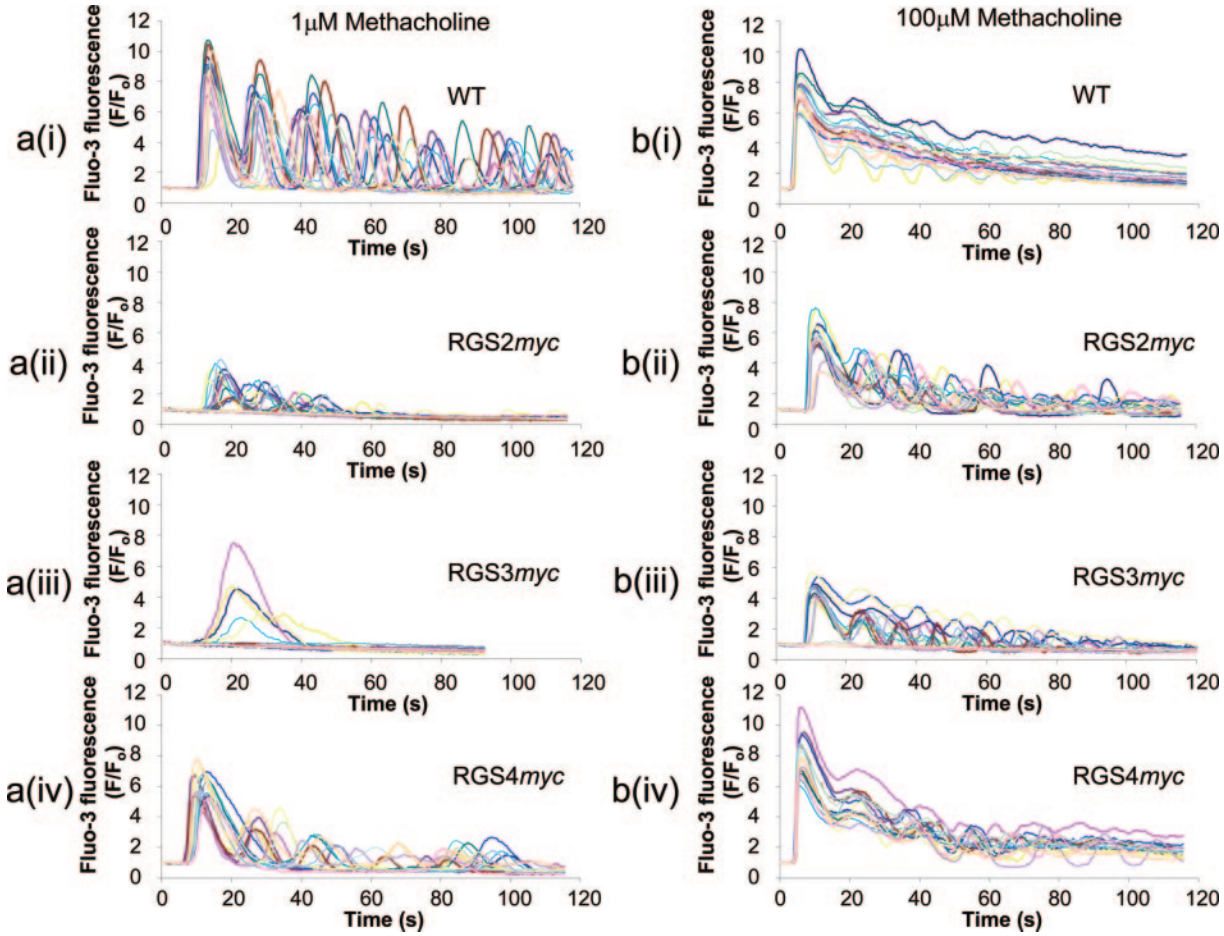

Fig. 8. RGS proteins alter the amplitude, kinetics, and pattern of Ca^{2+} signals generated by G$\alpha_{q/11}$-coupled receptors. a (i–iv), sample traces of Ca^{2+} responses seen in fluo-3 loaded cells [HEK293/WT (i), HEK293/RGS2*myc* (ii), HEK293/RGS3*myc* (iii), and HEK293/RGS4*myc* (iv)] in response to stimulation of the endogenous muscarinic M_3 receptor with a submaximal concentration of methacholine (1 μM). b(i–iv), sample traces as described in a(i–iv), but using a maximal concentration of methacholine (100 μM) as the stimulus. The traces illustrate responses from 15 to 20 cells from one field of view and are typical of traces obtained from at least four different coverslips.

ificity in vivo, and this could involve interactions with other molecules. An obvious candidate is the GPCR, as recently demonstrated for RGS2 and the third intracellular loop of the $G\alpha_{q/11}$-coupled muscarinic M_1 receptor (Bernstein et al., 2004). It is interesting that RGS2 but not RGS4 also interacts with this region of the muscarinic M_3 receptor (Bernstein et al., 2004). We were unable to obtain, however, any evidence for differences in the subcellular localization of the RGS proteins that could easily account for their different inhibitory properties. Thus, immunocytochemistry revealed that, as in previous studies (De Vries et al., 2000; Roy et al., 2003), RGS2*myc* is highly expressed in the nucleus, whereas both RGS3*myc* and RGS4*myc* are predominantly cytosolic.

To determine whether effector antagonism could account for RGS protein action, we examined their impact on GAP-resistant G-protein activation using either AlF_4^- to directly

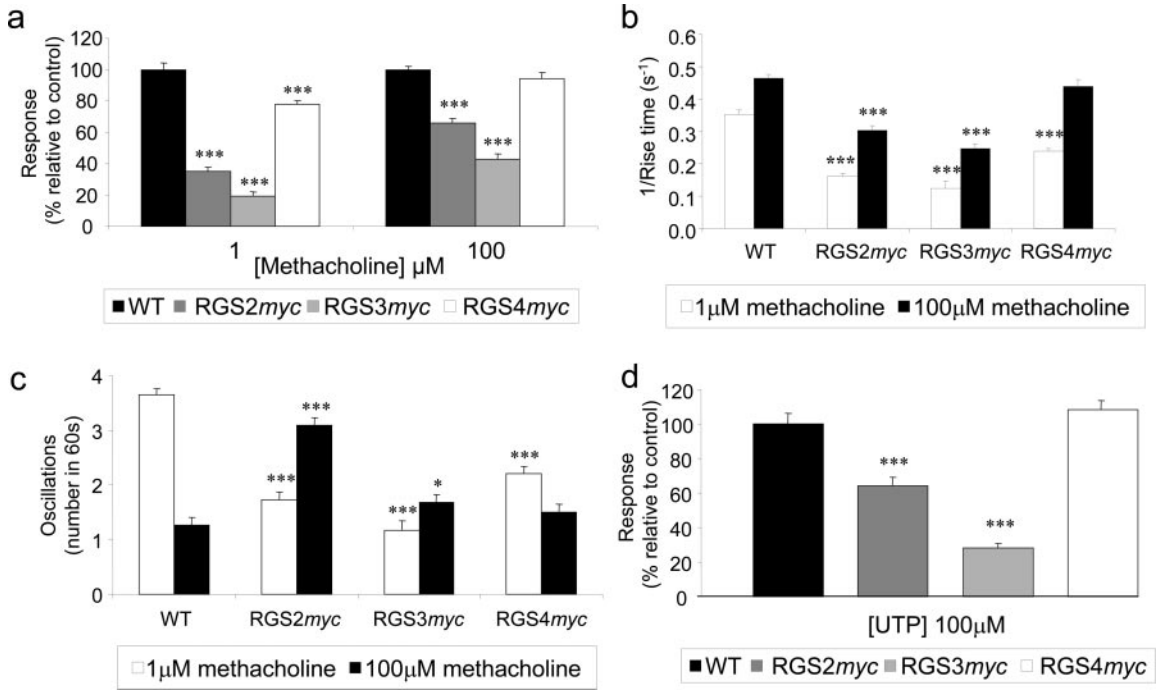

Fig. 9. RGS proteins alter the amplitude, kinetics and pattern of Ca^{2+} signals generated by $G\alpha_{q/11}$-coupled receptors: summary data. a, the effect of RGS*myc* protein expression on the amplitude of the initial Ca^{2+} transient generated in response to stimulation with either 1 or 100 μM methacholine. b, the effect of RGS protein expression on the kinetics of the initial Ca^{2+} response upon stimulation with 1 or 100 μM methacholine. Data are plotted as 1/rise time (s^{-1}), where the rise time was taken to be the time to reach a peak response from the initial point of inflection. c, the effect of RGS protein expression on Ca^{2+} oscillations generated in response to prolonged agonist stimulation (1 or 100 μM methacholine). Data represent the number of oscillations seen during a 60-s period after the initial Ca^{2+} response. d, the effect of RGS protein expression on the amplitude of the initial Ca^{2+} signal generated in response to stimulation of endogenous $P2Y_2$ receptors with 100 μM UTP. In all cases, the data represent the mean + S.E.M. for between 40 and 100 cells from at least four different coverslips. In a and d, data are expressed as the percentage response relative to control (HEK293/WT cells). Statistical comparisons were by one-way ANOVA with Dunnett's range test; ***, $P < 0.001$ versus control.

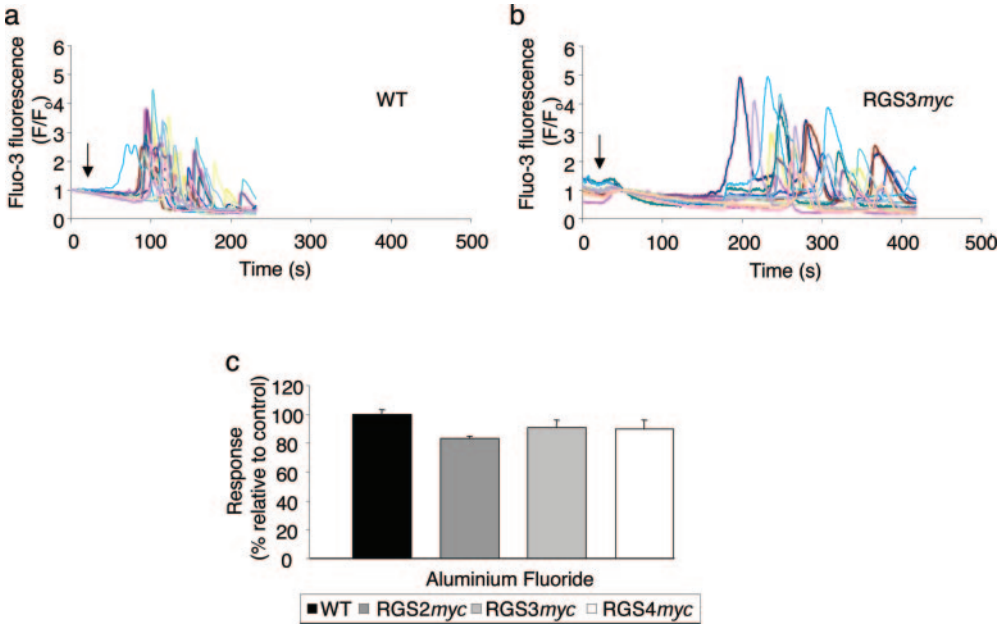

Fig. 10. RGS proteins do not alter the amplitude or pattern of Ca^{2+} signals generated by direct stimulation of G-proteins with AlF_4^-. a and b, sample traces of Ca^{2+} transients evoked by AlF_4^- stimulation of HEK293/WT and HEK293/RGS3*myc* cells, respectively. c, the effect of RGS protein expression on the amplitude of the initial Ca^{2+} signal generated in response to receptor-independent stimulation of G-proteins with AlF_4^-. Data represent the mean + S.E.M. for between 40 and 100 cells from at least four different coverslips.

activate G-proteins or a constitutively active $G\alpha_q$ (CA-$G\alpha_q$; Q209L) that is resistant to RGS protein GAP activity (Heximer et al., 2001). RGS protein expression did not affect AlF_4^--mediated [^{3}H]InsP_x accumulation. Furthermore, although RGS proteins increased the delay before AlF_4^--evoked Ca^{2+} oscillations, they did not affect either their frequency or amplitude. This suggests that GAP activity may be required to influence agonist-mediated oscillatory Ca^{2+} signals. The reason for the increased delay is unclear; it could reflect binding of RGS proteins to inactive G-protein α-subunits (Roy et al., 2003). Thus, the release of α-subunits could be delayed during AlF_4^- stimulation but not agonist stimulation, when the receptor acts as a guanine-nucleotide exchange factor (i.e., GDP-GTP exchange is not limiting). RGS proteins bind with higher affinity to G-proteins in the GDP-AlF_4^--bound state than the GTP-bound state (Ross and Wilkie, 2000), which may complicate interpretation. A final point limiting the usefulness of AlF_4^- is that it activates all heterotrimeric G-proteins, and those other than $G\alpha_{q/11}$ may contribute to the measured responses through, for example, the activation of PLC by G$\beta\gamma$-subunits. Thus, as an alternative approach, we used CA-$G\alpha_q$, which in addition to being GAP-resistant has an affinity for RGS proteins consistent with GTP-bound Gα-subunits (Ross and Wilkie, 2000), making it useful in the examination of effector antagonism. Transient transfection of CA-$G\alpha_q$ into HEK293/WT cells markedly increased PLC activity as judged from the accumulation of [^{3}H]InsP_x against a Li^+-block. Expression of CA-$G\alpha_q$ in the RGS*myc*-expressing cell lines similarly enhanced [^{3}H]InsP_x accumulation. Direct comparison of stimulation levels may be complicated by reciprocal effects of RGS proteins and Gα-subunits on expression levels (Anger et al., 2004). However, these data demonstrate that effector antagonism is insufficient to fully block G-protein-mediated activation of PLC. It is noteworthy that CA-$G\alpha_q$ caused robust accumulation of [^{3}H]InsP_x in RGS3*myc*-expressing cells despite almost no muscarinic receptor-mediated accumulation. Thus, RGS proteins were unable to efficiently block signaling by CA-$G\alpha_q$. Extrapolation to the effects of RGS proteins on endogenous G-proteins expressed at lower levels is difficult, and we cannot exclude the possibility that effector antagonism accounts for a proportion of the effects on receptor-mediated signaling. Indeed, a recent study suggested that GAP-independent mechanisms of RGS2 and RGS3 inhibited signaling by muscarinic M_3 receptors when overexpressed in COS-7 cells (Anger et al., 2004). However, the contribution of effector antagonism versus GAP activity for endogenously expressed RGS proteins acting on endogenously expressed receptors remains to be defined.

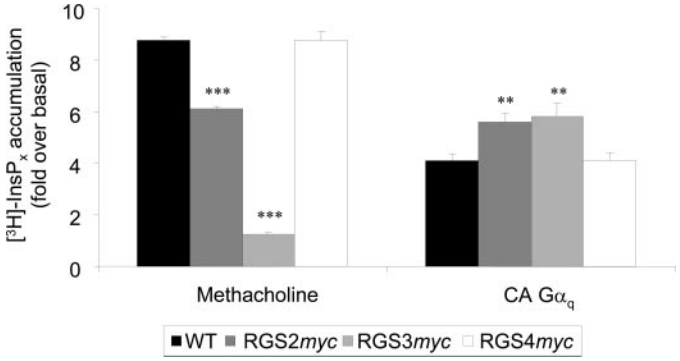

Fig. 11. The effect of RGS proteins on the activity of a constitutively active form of $G\alpha_q$ (CA-$G\alpha_q$). The accumulation of [^{3}H]InsP_x in HEK293/WT, HEK293/RGS2*myc*, HEK293/RGS3*myc*, and HEK293/RGS4*myc* transiently transfected with CA-$G\alpha_q$. Data represent the increase in [^{3}H]InsP_x accumulation over a 20-min period under Li^+-block in transfected cells compared with untransfected cells. Data are expressed as the mean + S.E.M. for three separate accumulations. Statistical comparisons were by one-way ANOVA with Dunnett's range test; **, $P < 0.01$; ***, $P < 0.001$ versus control.

In conclusion, along with population-based biochemical assays, we used a Ca^{2+}-sensitive dye and novel biosensors to detect $[Ca^{2+}]_i$, Ins(1,4,5)P_3, and diacylglycerol production to assess RGS-mediated inhibition of $G\alpha_{q/11}$-mediated signaling at the single-cell level in live cells and in real time. This allowed a detailed examination of the effects of RGS proteins on not only the magnitude of GPCR-mediated signaling but also the kinetics and temporal profiles.

References

Ancellin N, Preisser L, Le Maout S, Barbado M, Créminon C, Corman B, and Morel A (1999) Homologous and heterologous phosphorylation of the vasopressin V1a receptor. *Cell Signal* **11:**743–751.

Anger T, Zhang W, and Mende U (2004) Differential contribution of GTPase activation and effector antagonism to the inhibitory effect of RGS proteins on G_q-mediated signaling in vivo. *J Biol Chem* **279:**3906–3915.

Bernstein LS, Ramineni S, Hague C, Cladman W, Chidiac P, Levey AI, and Hepler JR (2004) RGS2 binds directly and selectively to the M1 muscarinic acetylcholine receptor third intracellular loop to modulate $G_{q/11}\alpha$ signaling. *J Biol Chem* **279:**21248–21256.

Castro-Fernandez C and Conn PM (2002) Regulation of the gonadotropin-releasing hormone receptor (GnRHR) by RGS proteins: role of the GnRHR carboxyl-terminus. *Mol Cell Endocrinol* **191:**149–156.

De Vries L, Zheng B, Fischer T, Elenko E, and Farquhar MG (2000) The regulator of G protein signaling family. *Annu Rev Pharmacol Toxicol* **40:**235–271.

Doupnik CA, Davidson N, Lester HA, and Kofuji P (1997) RGS proteins reconstitute the rapid gating kinetics of G$\beta\gamma$-activated inwardly rectifying K^+ channels. *Proc Natl Acad Sci (USA)* **94:**10461–10466.

Hepler JR (1999) Emerging roles for RGS proteins in cell signalling. *Trends Pharmacol Sci* **20:**376–382.

Heximer SP, Watson N, Linder ME, Blumer KJ, and Hepler JR (1997) RGS2/G0S8 is a selective inhibitor of Gqα function. *Proc Natl Acad Sci (USA)* **94:**14389–14393.

Heximer SP, Srinivasa SP, Bernstein LS, Bernard JL, Linder ME, Hepler JR, and Blumer KJ (1999) G protein selectivity is a determinant of RGS2 function. *J Biol Chem* **274:**34253–34259.

Heximer SP, Lim H, Bernard JL, and Blumer KJ (2001) Mechanisms governing subcellular localization and function of human RGS2. *J Biol Chem* **276:**14195–14203.

Hollinger S and Hepler JR (2002) Cellular regulation of RGS proteins: modulators and integrators of G protein signaling. *Pharmacol Rev* **54:**527–559.

Luo X, Popov S, Bera AK, Wilkie TM, and Muallem S (2001) RGS proteins provide biochemical control of agonist-evoked $[Ca^{2+}]_i$ oscillations. *Mol Cell* **7:**651–660.

Mitchell FM, Mullaney I, Godfrey PP, Arkinstall SJ, Wakelam MJO, and Milligan G (1991) Widespread distribution of Gqα/G11α detected immunologically by an antipeptide antiserum directed against the predicted C-terminal decapeptide. *FEBS Lett* **287:**171–174.

Nahorski SR, Young KW, Challiss RAJ, and Nash MS (2003) Visualizing phosphoinositide signalling in single neurons gets a green light. *Trends Neurosci* **26:**444–452.

Nash MS, Young KW, Willars GB, Challiss RA, and Nahorski SR (2001) Single-cell imaging of graded Ins(1,4,5)P_3 production following G-protein-coupled-receptor activation. *Biochem J* **356:**137–142.

Nash MS, Schell MJ, Atkinson PJ, Johnston NR, Nahorski SR, and Challiss RAJ (2002) Determinants of metabotropic glutamate receptor-5-mediated Ca^{2+} and inositol 1,4,5-trisphosphate oscillation frequency: receptor density versus agonist concentration. *J Biol Chem* **277:**35947–35960.

Neill JD, Duck LW, Sellers JC, Musgrove LC, Scheschonka A, Druey KM, and Kehrl JH (1997) Potential role for a regulator of G protein signaling (RGS3) in gonadotropin-releasing hormone (GnRH) stimulated desensitization. *Endocrinol* **138:**843–846.

Oancea E and Meyer T (1998) Protein kinase C as a molecular machine for decoding calcium and diacylglycerol signals. *Cell* **95:**307–318.

Oancea E, Teruel MN, Quest AF, and Meyer TJ (1998) Green fluorescent protein (GFP)-tagged cysteine-rich domains from protein kinase C as fluorescent indicators for diacylglycerol signaling in living cells. *J Cell Biol* **140:**485–498.

Ross EM and Wilkie TM (2000) GTPase-activating proteins for heterotrimeric G proteins: Regulators of G protein signaling (RGS) and RGS-like proteins. *Annu Rev Biochem* **69:**795–827.

Roy AA, Lemberg KE, and Chidiac P (2003) Recruitment of RGS2 and RGS4 to the plasma membrane by G proteins and receptors reflects functional interactions. *Mol Pharmacol* **64:**587–593.

Rumenapp U, Asmus M, Schablowski H, Woznicki M, Han L, Jakobs KH, Fahimi-Vahid M, Michalek C, Wieland T, and Schmidt M (2001) The M_3 muscarinic acetylcholine receptor expressed in HEK-293 cells signals to phospholipase D via

G_{12} but not G_q-type G proteins: regulators of G proteins as tools to dissect pertussis toxin-resistant G proteins in receptor-effector coupling. *J Biol Chem* **276:**2474–2479.

Scheschonka A, Dessauer CW, Sinnarajah S, Chidiac P, Shi CS, and Kehrl JH (2000) RGS3 is a GTPase-activating protein for $G_i\alpha$ and $G_q\alpha$ and a potent inhibitor of signaling by GTPase-deficient forms of $G_q\alpha$ and $G_{11}\alpha$. *Mol Pharmacol* **58:**719–728.

Snow BE, Krumins AM, Brothers GM, Lee SF, Wall MA, Chung S, Mangion J, Arya S, Gilman AG, and Siderovski DP (1998a) A G protein γ subunit-like domain shared between RGS11 and other RGS proteins specifies binding to $G\beta_5$ subunits. *Proc Natl Acad Sci (USA)* **95:**13307–13312.

Snow BE, Hall RA, Krumins AM, Brothers GM, Bouchard D, Brothers CA, Chung S, Mangion J, Gilman AG, Lefkowitz RJ, et al. (1998b) GTPase activating specificity of RGS12 and binding specificity of an alternatively spliced PDZ (PSD-95/Dlg/ZO-1) domain. *J Biol Chem* **273:**17749–17755.

Srinivasa SP, Watson N, Overton MC, and Blumer KJ (1998) Mechanism of RGS4, a GTPase-activating protein for G protein α subunits. *J Biol Chem* **273:**1529–1533.

Stauffer TP, Ahn S, and Meyer T (1998) Receptor-induced transient reduction in plasma membrane PtdIns(4,5)P_2 concentration monitored in living cells. *Curr Biol* **8:**343–346.

Tovey SC, de Smet P, Lipp P, Thomas D, Young KW, Missiaen L, De Smedt H, Parys JB, Berridge MJ, Thuring J, et al. (2001) Calcium puffs are generic $InsP_3$-activated elementary calcium signals and are downregulated by prolonged hormonal stimulation to inhibit cellular calcium responses. *J Cell Sci* **114:**3979–3989.

Werry TD, Christie MI, Dainty IA, Wilkinson GF, and Willars GB (2002) Ca^{2+} signalling by recombinant human CXCR2 chemokine receptors is potentiated by P2Y nucleotide receptors in HEK cells. *Br J Pharmacol* **135:**1199–1208.

Wheldon LM, Nahorski SR, and Willars GB (2001) Inositol 1,4,5-trisphosphate independent calcium signalling by platelet-derived growth factor in the human SH-SY5Y neuroblastoma cell. *Cell Calcium* **30:**95–106.

Willars GB, McArdle CA, and Nahorski SR (1998a) Acute desensitization of phospholipase C-coupled muscarinic M3 receptors but not gonadotropin-releasing hormone receptors co-expressed in αT3–1 cells: implications for mechanisms of rapid desensitization. *Biochem J* **333:**301–308.

Willars GB and Nahorski SR (1995) Quantitative comparisons of muscarinic and bradykinin receptor-mediated Ins(1,4,5)P_3 accumulation and Ca^{2+} signalling in human neuroblastoma cells. *Br J Pharmacol* **114:**1133–1142.

Willars GB, Nahorski SR, and Challiss RAJ (1998b) Differential regulation of muscarinic acetylcholine receptor-sensitive polyphosphoinositide pools and consequences for signaling in human neuroblastoma cells. *J Biol Chem* **273:**5037–5046.

Witherow DS, Wang Q, Levay K, Cabrera JL, Chen J, Willars GB, and Slepak VZ (2000) Complexes of the G protein subunit $G\beta_5$ with the regulators of G protein signaling RGS7 and RGS9. Characterization in native tissues and in transfected cells. *J Biol Chem* **275:**24872–24880.

Witherow DS, Tovey SC, Wang Q, Willars GB, and Slepak VZ (2003) Gβ5·RGS7 inhibits $G\alpha_q$-mediated signaling via a direct protein-protein interaction. *J Biol Chem* **278:**21307–21313.

Xu X, Zeng W, Popov S, Berman DM, Davignon I, Yu K, Yowe D, Offermanns S, Muallem S, and Wilkie TM (1999) RGS proteins determine signaling specificity of G_q-coupled receptors. *J Biol Chem* **274:**3549–3556.

Zeng W, Xu X, Popov S, Mukhopadhyay S, Chidiac P, Swistokl J, Danho W, Yagaloff KA, Fisher SL, Ross EM, et al. (1998) The N-terminal domain of RGS4 confers receptor-selective inhibition of G protein signaling. *J Biol Chem* **273:**34687–34690.

Zheng B, De Vries L, and Gist Farquhar M (1999) Divergence of RGS proteins: evidence for the existence of six mammalian RGS subfamilies. *Trends Biochem Sci* **24:**411–414.

Address correspondence to: Dr. Gary B. Willars, Department of Cell Physiology and Pharmacology, Medical Sciences Building, University of Leicester, University Road, LE1 9HN, United Kingdom. E-mail: gbw2@le.ac.uk